Reduction of spillover effects on independent modal space control through optimal placement of sensors and actuators

S Cinquemani, D Ferrari and I Bayati

Politecnico di Milano, Dipartimento di Meccanica, Campus Bovisa Sud, via La Masa 1, 20156, Milano, Italy

E-mail: simone.cinquemani@polimi.it

Received 18 December 2014, revised 3 April 2015
Accepted for publication 6 May 2015
Published 2 July 2015

1. Introduction

The main focus of the modal control approach is that the coupled equations of motion of a dynamic system can be decoupled in the modal space, so that modal control forces can be independently designed for each mode through feedback control. The very first investigations on this topic [1, 2, 19] are usually taken as reference in modal control techniques applied to the control of vibrations in flexible structural systems in general. In these works, the state variable feedback, modal control, and optimal control techniques are referred to as active control. However, when it comes to controlling real dynamic systems, achieving this task can be troublesome and stability cannot be guaranteed *a priori* even for the controlled modes.

Although modal control techniques are simple to design and are not demanding in terms of computational effort [20], they have some disadvantages such as the need for a high number of sensors and actuators to be placed on the vibrating structure [3]. However, these limits could be considered less burdensome if new technologies, such as optical strain gauges [6–8], are adopted.

A variety of modal control algorithms has been specifically developed for civil engineering structures [10, 11], and mechanical [5] and aerospace systems [15, 18]. However, the great potential of the independent modal space control (IMSC) technique has not been fully exploited yet, mainly because of problems related to spillover effects. A few works have suggested containing spillover effects by using modal filters on measurements. This can be achieved by using filters on signals [3, 21, 25] or using modal sensors [23, 24]. A trade-off between these two approaches can be found in [8] and [26]. Unfortunately, although these approaches can reduce observation spillover, control spillover still remains.

A few works [9, 16, 17] have studied the dependence of spillover effects on the mutual positions of actuators and sensors when IMSC is applied. However, these studies are

based on very complex mathematical approaches which cannot easily be applied within ordinary engineering practice.

This paper addresses the problem with a rigorous approach, even evaluating the physical connection of the analytical terms involved in the modeling process. More specifically, we show how the stability of independent modal control can be directly diagnosed and how spillover effects can be adequately limited by a suitable choice for the loca-tions of sensors and actuators. This choice follows an opti-mization approach: the global minimum of a proper single-objective cost function was sought using a genetic algorithm. Genetic algorithms were adopted for their consistent applic-ability in cases where the cost functions are not analytically derivable, as in this case. The implementation of these algo-rithms usually requires only a limited number of iterations to converge to the optimal solution and is definitely much more straightforward than investigating each possible solution separately.

This paper is structured as follows: section 2 recalls the basics of the modal control of an n-degrees of freedom (DOF) mechanical system and section 3 shows how it is possible to evaluate the effects of control by analyzing the modal damping matrix of the controlled system. In section 4 the objective function is introduced to minimize spillover effects. Theoretical aspects are supported by numerical simulations carried out under different conditions (section 5). Some results of preliminary experimental tests are discussed in section 6. Finally, our conclusions are reported in section 7.

2. Modal control of a mechanical system

The modal control method is based on the idea of coordinate transformations, whereby the system is decoupled into a set of independent second order systems in terms of modal coordinates. As a result, the control system design can be carried out for each second-order system independently, no matter how large the model is. The equations of motion of a n-DOF system in terms of modal coordinates are:

$$[\mathbf{M}]\ddot{\underline{\mathbf{q}}}(t) + [\mathbf{R}]\dot{\underline{\mathbf{q}}}(t) + [\mathbf{K}]\underline{\mathbf{q}}(t) = \left[\boldsymbol{\phi}\left(\underline{\boldsymbol{\xi}}_D\right)\right]^{\mathrm{T}}\underline{\mathbf{F}}_{\mathrm{D}}(t). \quad (1)$$

where the matrices **[M]**, **[R]** and **[K]** are, respectively, $n \times n$ modal mass, modal damping and modal stiffness matrices, that can be written as functions of [**M***], [**R***] and [**K***], which are $n \times n$ physical mass, damping and stiffness matrices and [$\boldsymbol{\phi}$], which is the system's modal matrix [22]. $\mathbf{F}_{\mathrm{D}}(t)$_ is the $n_{\mathrm{D}} \times 1$ disturbance forces and $\left[\boldsymbol{\phi}\left(\underline{\boldsymbol{\xi}}_D\right)\right]^{\mathrm{T}}$ is the transposed modal matrix evaluated in points of application of disturbance forces ($\underline{\boldsymbol{\xi}}_{\mathrm{D}}$).

Due to the orthogonality of modes, [**M**], [**R**] and [**K**] are diagonal. and modes are uncoupled. The equation of motion of each mode can be expressed as:

$$m_i\ddot{q}_i + r_i\dot{q}_i + k_i q_i = \underline{\boldsymbol{\phi}}_i^{\mathrm{T}}\left(\underline{\boldsymbol{\xi}}_{\mathrm{D}}\right)\underline{\mathbf{F}}_{\mathrm{D}}(t). \quad (2)$$

A complete dynamical model of the vibrating system is usually not available or, even if it could be achieved through finite element analysis (FEA), it could not been used to design the control law. This operation is usually carried out on a reduced model of the system, characterized by a finite number of modes $n_{\mathrm{R}} < n$. The reduced model can be achieved in the following two ways: FEA and experimental modal identification techniques. The reduced model is valid only in the range of frequencies where it can suitably describe the behavior of the real system. In the following the modes described in the reduced model are referred to as *modeled modes*, with respect to those of the real system which are referred to as *real modes*. Real modes, which are not included in the modeled ones, will be referred as to *unmodeled modes*. Equation (1) becomes:

$$\left[\tilde{\mathbf{M}}\right]\ddot{\underline{\mathbf{q}}}_{\mathrm{R}}(t) + \left[\tilde{\mathbf{R}}\right]\dot{\underline{\mathbf{q}}}_{\mathrm{R}}(t) + \left[\tilde{\mathbf{K}}\right]\underline{\mathbf{q}}_{\mathrm{R}}(t) = \left[\tilde{\boldsymbol{\phi}}\left(\underline{\boldsymbol{\xi}}_D\right)\right]^{\mathrm{T}}\underline{\mathbf{F}}_{\mathrm{D}}(t) + \left[\tilde{\boldsymbol{\phi}}\left(\underline{\boldsymbol{\xi}}_C\right)\right]^{\mathrm{T}}\underline{\mathbf{F}}_{\mathrm{C}}(t) \quad (3)$$

where $\left[\tilde{\mathbf{M}}\right]$, $\left[\tilde{\mathbf{R}}\right]$ and $\left[\tilde{\mathbf{K}}\right]$ are, respectively, the $n_{\mathrm{R}} \times n_{\mathrm{R}}$ modal mass, modal damping and modal stiffness matrices of the reduced model; $\underline{\mathbf{q}}_{\mathrm{R}}$ is the $n_{\mathrm{R}} \times 1$ vector of the modal displacements of the modeled modes and $[\tilde{\boldsymbol{\phi}}(\underline{\boldsymbol{\xi}}_D)]^{\mathrm{T}}$ and $[\tilde{\boldsymbol{\phi}}(\underline{\boldsymbol{\xi}}_C)]^{\mathrm{T}}$ are the modal matrix evaluated, respectively, in terms of the points of application of disturbance and control forces limited to the modeled modes.

Both modal identification techniques and FEA allow one to evaluate $\left[\tilde{\mathbf{M}}\right]$, $\left[\tilde{\mathbf{R}}\right]$, $\left[\tilde{\mathbf{K}}\right]$, $\left[\tilde{\boldsymbol{\phi}}\left(\underline{\boldsymbol{\xi}}_D\right)\right]$ and $\left[\tilde{\boldsymbol{\phi}}\left(\underline{\boldsymbol{\xi}}_C\right)\right]$ [22]. Equation (3) can be expressed for the ith modeled mode as:

$$m_i\ddot{q}_{r,i} + r_i\dot{q}_{r,i} + k_i q_{r,i} = \underline{\boldsymbol{\phi}}_i^{\mathrm{T}}\left(\underline{\boldsymbol{\xi}}_{\mathrm{D}}\right)\underline{\mathbf{F}}_{\mathrm{D}}(t) + \underline{\boldsymbol{\phi}}_i^{\mathrm{T}}\left(\underline{\boldsymbol{\xi}}_{\mathrm{C}}\right)\underline{\mathbf{F}}_{\mathrm{C}}(t). \quad (4)$$

Naturally, modeled modes still remain uncoupled if, and only if:

$$\underline{\boldsymbol{\phi}}_i^{\mathrm{T}}\left(\underline{\boldsymbol{\xi}}_{\mathrm{C}}\right)\underline{\mathbf{F}}_{\mathrm{C}}(t) = f\left(\ddot{q}_{r,i}, \dot{q}_{r,i}, q_{r,i}\right). \quad (5)$$

2.1. Observability and controllability

Using a modal approach it is straightforward to verify the controllability of the system by observing the Lagrangian components of the control forces with respect to the modal coordinates. Referring to (4) this means that, for each controlled mode, this must be:

$$\underline{\boldsymbol{\phi}}_i^{T}\left(\underline{\boldsymbol{\xi}}_{\mathrm{C}}\right)\underline{\mathbf{F}}_{\mathrm{C}}(t) \neq 0 \quad \text{for} \quad i = 1,...,n_{\mathrm{C}} \quad (6)$$

where n_{C} is referred to as the number of controlled modes. Physically, this corresponds to having, for each controlled mode, at least one actuator which is not placed in a node of the considered mode. Since $[\boldsymbol{\phi}]^{\mathrm{T}}$ in equation (1) has to be

invertible, it has to be

$$\det\left[\boldsymbol{\phi}\left(\underline{\boldsymbol{\xi}}_C\right)\right] \neq 0. \tag{7}$$

Modal velocities $\dot{\underline{\mathbf{q}}}_R$ can be calculated from measurements of physical displacements, velocities or accelerations. Let us assume that m sensors and points of measurement are available. Modal velocities can be hypothesized as:

$$\dot{\underline{\mathbf{q}}}_{\mathrm{R}} = \left[\tilde{\boldsymbol{\phi}}\left(\underline{\boldsymbol{\xi}}_M\right)\right]^{-1}\dot{\underline{\mathbf{z}}} \tag{8}$$

where $\left[\tilde{\boldsymbol{\phi}}\left(\underline{\boldsymbol{\xi}}_M\right)\right]$ is a $n_{\mathrm{R}} \times m$ matrix, obtained from modal matrix of the reduced model limited to points where sensors are located ($\underline{\boldsymbol{\xi}}_M$). Equation (8) highlights how contributions of unmodeled modes on measurements are neglected. Since $\left[\tilde{\boldsymbol{\phi}}\left(\underline{\boldsymbol{\xi}}_M\right)\right]$ must be invertible, $m \geqslant n_{\mathrm{R}}$.

3. Effects of control

An effective way to reduce vibration is to design control forces to increase the modal damping of modeled modes. According to [4] modal control forces have to be proportional and in-phase with the corresponding modal velocities. Let us assume that n_{C} actuators equal to the number of modeled modes ($n_{\mathrm{C}} = n_{\mathrm{R}}$) are available. The modal control forces are designed to be:

$$\left[\boldsymbol{\phi}\left(\underline{\boldsymbol{\xi}}_C\right)\right]^{\mathrm{T}}\underline{\mathbf{F}}_{\mathrm{C}}(t) = -\left[\tilde{\mathbf{r}}\right]\dot{\underline{\mathbf{q}}}_{\mathrm{R}} \tag{9}$$

where $\left[\tilde{\mathbf{r}}\right]$ is the matrix of damping gains introduced by the control law.

Physical control forces can be calculated from equation (9). Note how $\left[\tilde{\boldsymbol{\phi}}\left(\underline{\boldsymbol{\xi}}_C\right)\right]$ is an $n_{\mathrm{A}} \times n_{\mathrm{R}}$ matrix, n_{A} being the number of actuators. To invert it, a number of actuators equal to the number of modeled modes is required ($n_{\mathrm{A}} = n_{\mathrm{R}}$).

In this case, the physical control forces vector $\underline{\mathbf{F}}_{\mathrm{C}}$ can be obtained from equation (9), so that:

$$\underline{\mathbf{F}}_{\mathrm{C}} = -\left[\tilde{\boldsymbol{\phi}}\left(\underline{\boldsymbol{\xi}}_C\right)\right]^{-\mathrm{T}}\left[\tilde{\mathbf{r}}\right]\dot{\underline{\mathbf{q}}}_{\mathrm{R}}. \tag{10}$$

Despite the modal control forces being designed to suppress vibration related to modeled modes, when they are applied to the real system in equation (1), they can drive all real modes (control spillover).

Combining equations (8) and (10) and recalling that the physical coordinates $\dot{\underline{\mathbf{z}}}$ are linked to modal ones by the modal matrix, the control force vector $\underline{\mathbf{F}}_{\mathrm{C}}$, expressed as a function of modal velocities, is:

$$\underline{\mathbf{F}}_{\mathrm{C}} = -\left[\tilde{\boldsymbol{\phi}}\left(\underline{\boldsymbol{\xi}}_C\right)\right]^{-\mathrm{T}}\left[\tilde{\mathbf{r}}\right]\left[\tilde{\boldsymbol{\phi}}\left(\underline{\boldsymbol{\xi}}_M\right)\right]^{-1}\left[\boldsymbol{\phi}\left(\underline{\boldsymbol{\xi}}_M\right)\right]\dot{\underline{\mathbf{q}}}. \tag{11}$$

The observation spillover effect is evident in equation (11). Control forces $\underline{\mathbf{F}}_{\mathrm{C}}$ cannot really be a function of only modeled modes, they are also influenced by unmodeled ones. The term $\left[\tilde{\boldsymbol{\phi}}\left(\underline{\boldsymbol{\xi}}_M\right)\right]^{-1}\left[\boldsymbol{\phi}\left(\underline{\boldsymbol{\xi}}_M\right)\right]$ in equation (11) is representative of such an effect.

Observation spillover can be conveniently limited in the range of frequency where the reduced model (and then the modeled modes) correctly reproduces the behavior of the real system.

Substituting equation (11) in (1) and (3) the equations of motion of the reduced model are:

$$\begin{aligned}&\left[\tilde{\mathbf{M}}\right]\ddot{\underline{\mathbf{q}}}_{\mathrm{R}}(t) + \left[\tilde{\mathbf{R}}\right]\dot{\underline{\mathbf{q}}}_{\mathrm{R}}(t) + \left[\tilde{\mathbf{K}}\right]\underline{\mathbf{q}}_{\mathrm{R}}(t)\\ &= \left[\tilde{\boldsymbol{\phi}}\left(\underline{\boldsymbol{\xi}}_D\right)\right]^{\mathrm{T}}\underline{\mathbf{E}}_{\mathrm{D}}(t) - \left[\tilde{\boldsymbol{\phi}}\left(\underline{\boldsymbol{\xi}}_C\right)\right]^{\mathrm{T}}\left[\tilde{\boldsymbol{\phi}}\left(\underline{\boldsymbol{\xi}}_C\right)\right]^{-\mathrm{T}}\left[\tilde{\mathbf{r}}\right]\dot{\underline{\mathbf{q}}}_{\mathrm{R}}\end{aligned} \tag{12}$$

while for the real system (modeled and unmodeled modes):

$$\begin{aligned}&[\mathbf{M}]\ddot{\underline{\mathbf{q}}}(t) + [\mathbf{R}]\dot{\underline{\mathbf{q}}}(t) + [\mathbf{K}]\underline{\mathbf{q}}(t) = \left[\boldsymbol{\phi}\left(\underline{\boldsymbol{\xi}}_D\right)\right]^{\mathrm{T}}\underline{\mathbf{E}}_{\mathrm{D}}(t)\\ &-\left[\boldsymbol{\phi}\left(\underline{\boldsymbol{\xi}}_C\right)\right]^{\mathrm{T}}\left[\tilde{\boldsymbol{\phi}}\left(\underline{\boldsymbol{\xi}}_C\right)\right]^{-\mathrm{T}}\left[\tilde{\mathbf{r}}\right]\left[\tilde{\boldsymbol{\phi}}\left(\underline{\boldsymbol{\xi}}_M\right)\right]^{-1}\left[\boldsymbol{\phi}\left(\underline{\boldsymbol{\xi}}_M\right)\right]\dot{\underline{\mathbf{q}}}.\end{aligned} \tag{13}$$

The effect of the control law on the system damping is visible in the gathering of modal velocities for both the reduced and the complete model:

$$\begin{aligned}&\left[\tilde{\mathbf{M}}\right]\ddot{\underline{\mathbf{q}}}_{\mathrm{R}}(t) + \left(\left[\tilde{\mathbf{R}}\right] + \left[\tilde{\mathbf{R}}_C\right]\right)\dot{\underline{\mathbf{q}}}_{\mathrm{R}}(t)\\ &\quad + \left[\tilde{\mathbf{K}}\right]\underline{\mathbf{q}}_{\mathrm{R}}(t) = \left[\tilde{\boldsymbol{\phi}}\left(\underline{\boldsymbol{\xi}}_D\right)\right]^{\mathrm{T}}\underline{\mathbf{E}}_{\mathrm{D}}(t)\end{aligned} \tag{14}$$

$$\begin{aligned}&[\mathbf{M}]\ddot{\underline{\mathbf{q}}}(t) + \left([\mathbf{R}] + \left[\mathbf{R}_{\mathbf{C}}\right]\right)\dot{\underline{\mathbf{q}}}(t) + [\mathbf{K}]\underline{\mathbf{q}}(t)\\ &= \left[\boldsymbol{\phi}\left(\underline{\boldsymbol{\xi}}_D\right)\right]^{\mathrm{T}}\underline{\mathbf{E}}_{\mathrm{D}}(t)\end{aligned} \tag{15}$$

where

$$\left[\tilde{\mathbf{R}}_C\right] = \left[\tilde{\boldsymbol{\phi}}\left(\underline{\boldsymbol{\xi}}_C\right)\right]^{\mathrm{T}}\left[\tilde{\boldsymbol{\phi}}\left(\underline{\boldsymbol{\xi}}_C\right)\right]^{-\mathrm{T}}\left[\tilde{\mathbf{r}}\right] = \left[\tilde{\mathbf{r}}\right] \tag{16}$$

is the damping matrix introduced by the control law on the reduced model.

Designing the matrix $\left[\tilde{\mathbf{r}}\right]$ as diagonal, the controlled modes become uncoupled since an extra-diagonal element is present. This result is independent of the position of actuators and sensors. Considering only the reduced model, the independent modal control seems to be highly effective on the modeled modes and is stable for both the collocated and non-collocated control.

However, looking at the real system, the damping matrix introduced by the control is:

$$\begin{aligned}\left[\mathbf{R}_{\mathbf{C}}\right] &= \underbrace{\left[\boldsymbol{\phi}\left(\underline{\boldsymbol{\xi}}_C\right)\right]^{\mathrm{T}}\left[\tilde{\boldsymbol{\phi}}\left(\underline{\boldsymbol{\xi}}_C\right)\right]^{-\mathrm{T}}}_{\text{Control spillover}}\\ &\quad\cdot\left[\tilde{\mathbf{r}}\right]\underbrace{\left[\tilde{\boldsymbol{\phi}}\left(\underline{\boldsymbol{\xi}}_M\right)\right]^{-1}\left[\boldsymbol{\phi}\left(\underline{\boldsymbol{\xi}}_M\right)\right]}_{\text{Observation spillover}}\\ &= \begin{bmatrix}\left[\tilde{r}\right]_{n_{\mathrm{R}}\times n_{\mathrm{R}}} & r_{i,j}\\ r_{j,i} & \ddots\end{bmatrix}_{n\times n}.\end{aligned} \tag{17}$$

From equation (17) it can be noted that, even assuming the gain matrix $[\bar{\mathbf{r}}]$ as diagonal, the system is characterized by a total damping matrix that is no longer diagonal. The extra-diagonal terms $r_{i,j}$ and $r_{j,i}$ (generally non null) can be considered as representative of spillover effects. They couple the equations of motion of the real modes and they can affect the stability of the controlled system and the performance itself. Equation (17) gives the first analytical relationship between spillover effects for IMSC and the positions of sensors and actuators on the flexible structure.

4. Limiting spillover effects

System stability can be improved by properly designing the modal damping matrix of the real controlled system equation (17). To guarantee the stability of the control law, the matrix $[\mathbf{R_C}]$ is required to be positive-definite and should also be symmetric to avoid possible dynamic instabilities. Considering equation (17), matrix $[\mathbf{R_C}]$ is symmetric if, and only if, it is:

$$\begin{aligned}&\left[\boldsymbol{\phi}\left(\underline{\xi}_C\right)\right]^{\mathrm{T}}\left[\tilde{\boldsymbol{\phi}}\left(\underline{\xi}_C\right)\right]^{-\mathrm{T}}[\bar{\mathbf{r}}]\left[\tilde{\boldsymbol{\phi}}\left(\underline{\xi}_M\right)\right]^{-1}\left[\boldsymbol{\phi}\left(\underline{\xi}_M\right)\right]\\ &=\left[\boldsymbol{\phi}\left(\underline{\xi}_M\right)\right]^{\mathrm{T}}\left[\tilde{\boldsymbol{\phi}}\left(\underline{\xi}_M\right)\right]^{-\mathrm{T}}[\bar{\mathbf{r}}]\left[\tilde{\boldsymbol{\phi}}\left(\underline{\xi}_C\right)\right]^{-1}\left[\boldsymbol{\phi}\left(\underline{\xi}_C\right)\right]\end{aligned} \quad (18)$$

which is true only for collocated control ($\underline{\xi}_{\mathbf{C}} = \underline{\xi}_{\mathbf{M}}$).

Vice versa, if the control is non-collocated, even if the damping matrix of the reduced model is diagonal, spillover effects can threaten the system's stability.

As spillover effects can be interpreted as the presence of non-diagonal elements of $[\mathbf{R_C}]$ and they depend only on the positions of the actuators and sensors, it is reasonable to assume that a suitable choice of their positions could enhance the performance of the control, limiting undesired effects.

The idea to reduce spillover is simple: if one could place the actuators exerting control forces and the sensors on the nodes of the unmodeled modes, spillover effects would be zero. Physically this means that the control forces are not able to drive unmodeled modes and sensors are not able to measure quantities related to unmodeled modes. Analytically, this means that the extra-diagonal terms of the matrix $[\mathbf{R_C}]$ would be equal to zero. It should be stated that the theoretical goal related to the control of flexible systems is that the amount of energy introduced should be totally exploited to control only the controlled modes of vibration. Such an objective is unrealistic because there are no points on the structure which are nodes of all the unmodeled vibrational modes. However, one can choose some places on the system that minimize the amount of energy introduced into unmodeled modes, obviously preserving the system observability and controllability.

One should aim to reduce $r_{c_{i,j}}$ as much as possible, potentially to zero, by means of an optimal positioning of sensors and actuators. This is a very challenging task which could be achieved only in the sense of minimizing the spillover effect.

4.1. Fitness function

Let us assume that the n modes of a real system are known. Suppose then that we aim to control the first n_{R} modes of the system and then define the reduced model to synthesize the IMSC. To use this approach a number of actuators $n_{\mathrm{C}} = n_{\mathrm{R}}$ and a number of sensors $m = n_{\mathrm{R}}$ have to be used.

A fitness function can be introduced as the sum of the absolute values of the extra-diagonal elements of the damping matrix $[\mathbf{R_C}]$:

$$f\left(\underline{\xi}_{\mathbf{C}}, \underline{\xi}_{\mathbf{M}}\right) = \sum_{i \neq j}\left|\mathbf{R}_{\mathbf{C},ij}\right|. \quad (19)$$

This function has to be minimized through an optimal placement of sensors and actuators.

The real system is subdivided into N points where sensors and actuators can be placed. The modal matrix is then a $N \times n$ matrix, where the ith row corresponds to the values of the modal shapes evaluated for the point i of the system. The choice of the positions of both the sensors and actuators corresponds to choosing the corresponding row of the modal matrix. The positions of the actuators and sensors are then collected in $\underline{\xi}_{\mathbf{C}}$ and $\underline{\xi}_{\mathbf{M}}$.

Two different control types are considered: collocated control and non-collocated control. In the former the actuators and the sensors are constrained to have the same position $\underline{\xi}_{\mathbf{C}} = \underline{\xi}_{\mathbf{M}}$, so that the number of parameters to optimize is $n_{\mathrm{p}} = n_{\mathrm{R}}$. In the latter the actuators can occupy different nodes with respect to the sensors $\underline{\xi}_{\mathbf{C}} \neq \underline{\xi}_{\mathbf{M}}$, so that the number of parameters to optimize is $n_{\mathrm{p}} = 2n_{\mathrm{R}}$.

4.2. Optimization method

Seeking the global minimum of the fitness function previously defined means solving a single-objective optimization problem, for which the genetic algorithm can be used, as explained in detail in the pioneering work [12], as well as in [13]. One of the main advantages of genetic algorithms is the possibility to solve non-smooth problems when the fitness function, as in this case, does not have derivable properties and gradient-based methods are therefore not suitable [14].

The fitness function maps the space of the n_{p} parameters to be optimized, called *the decision space*, into the space of the objectives, which is a one-dimensional space in this work. The boundary of the decision space is fixed by setting the lower bound (lb) and the upper bound (ub) for each parameter. Within the decision space, the subset which meets all the constraint relations is called *the feasible space*. In this work, all the parameters can vary from 1 to N, because each of them represents a row of the modal matrix $[\phi]$, while the constraints are:

- $\det\left[\tilde{\phi}\left(\underline{\xi}_{\mathbf{C}}\right)\right] \neq 0$, for system controllability;
- $\det\left[\tilde{\phi}\left(\underline{\xi}_{\mathbf{M}}\right)\right] \neq 0$, for system observability.

In the case of collocated control, the first two constrains coincide. They also forbid the possibility of two or more actuators, or sensors, occupying the same node of the system.

To implement the constraint relations, appropriate thresholds c_1, c_2 have to be chosen:

- $\text{cond}\left[\tilde{\phi}\left(\underline{\xi}_{\mathbf{C}}\right)\right] < c_1$;
- $\text{cond}\left[\tilde{\phi}\left(\underline{\xi}_{\mathbf{M}}\right)\right] < c_2$;

where 'cond' is referred to as the matrix condition number, defined as the ratio between the maximum and the minimum eigenvalue of the matrix $[\tilde{\phi}]$, being an index of the stability of the numerical solution due to small variation in the input data. The genetic algorithm is based on a natural selection process that mimics biological evolution and it works by iteratively producing new generations in terms of individuals covering the decision space as much as possible, consistent with the constraints, and keeping the best individuals (*elite*) over the iterations, according to proper weighting functions. In addition to elite individuals, *crossover* combination is also possible, so that the child is produced by random combination of the genes of two parent individuals, whose values remain unchanged over the generations, in addition to *mutation*, the child being produced by random mutation of the genes of a single parent individual.The algorithm stops at this point if the weighted average of the difference in the minimum value of the objective, computed on the so-called N_s stall generations, is less than the tolerance.

In a second step the constraint handling is introduced. Constraints are integrated in the fitness function, so that, in the case of violations, the objective is set equal to a fixed high value, which is chosen to be sufficiently larger than the maximum fitness function evaluation detected among the feasible individuals.

The stopping criterion is based on a tolerance threshold and takes into account N_s stall generations prior to the current one, the number of which is chosen by the user. One can also set different criteria, such as the achievement of a maximum number of generations, or a maximum time limit, or a lower limit of the fitness function value. The algorithm stops as soon as one of these conditions is met.

A key feature of genetic algorithms is the preservation of so-called *diversity* between parameters in the production of the children. It represents the average distance among individuals of a population in the decision space and in the objective space. The maintenance of the diversity among individuals, from generation to generation, is essential because it allows the algorithm to search for the optimum in as wide a region as possible. This is the reason why the average of the fitness function evaluations does not show any descending trend over iterations. However, a more detailed description of the algorithm reported herein can be found in [12, 13].

5. Numerical simulations

In order to evaluate the effects of the positions of the sensors and actuators on the control and to evaluate the performance of the genetic algorithm in reducing spillover effects, some numerical simulations have been carried out. Let us consider a squared flexible plate whose main mechanical parameters [**M**], [**R**] and [**K**] have been obtained through a finite element model. Let us assume that the control of modes 1, 2 and 3 is required along with suppressing the vibration of the modeled modes by increasing their damping of a given quantity defined by the gain matrix $\left[\bar{r}\right]$. A reduced model of the system can be obtained by considering only the first three modes, whereas the others can be considered as unmodeled.

Table 1. The main parameters used for the numerical simulations.

System: two-dimensional plate	
N	$56 \times 56 = 3.136$
n	10
$n_R = n_C = m$	3 (modes: 1, 2, 3)
$[\tilde{r}]$	$5 \cdot I_{3\times3}$ (Ns m^{-1})
Genetic algorithm `ga.m`	
Population size	135
Max. generations	10.000
Stall generations	10.000
Tolerance	10^{-16} (`eps`)
Threshold c_1	10^3
Threshold c_2	10^3
Computational resources	
Matlabpool size	4
CPU type	quad-core 2, 40 GHz
CPU utilization	25%

For each test, the positions of both the sensors and actuators are optimized to limit spillover effects. The performance of the system will be evaluated by looking at the poles of the controlled system. Table 1 gives an overview of the main parameters used for the genetic algorithm optimization. The

5.1. Test 1—(n = 4) collocated control

The first test was carried out on a simple system characterized by four modes ($n = 4$). Needless to say, this very simple case would not require any optimization technique; nevertheless, it is a straightforward and useful tool to check the validity of the proposed technique. Figure 1 shows the real part of the poles of both the uncontrolled (using the symbol $*$) and controlled systems with genetic algorithm optimization (using the symbol $\circ$). For the unmodeled mode (the 4th mode), the box-plot provides the median value of the real part of the poles of the controlled systems for all the possible combinations of unoptimized positions of sensors and actuators. The ends of the box-plot correspond to the 25th and 75th percentiles. It should be noted that, whenever the optimization algorithm is used, the pole of the unmodeled mode is unchanged, thus confirming that there are no spillover effects. This result can be easily obtained by placing sensors and actuators on the nodes of the unmodeled mode (see figure 2). In contrast, if their position is random, spillover effects can change the pole of the unmodeled mode. However, as the control is collocated, the system is always stable.

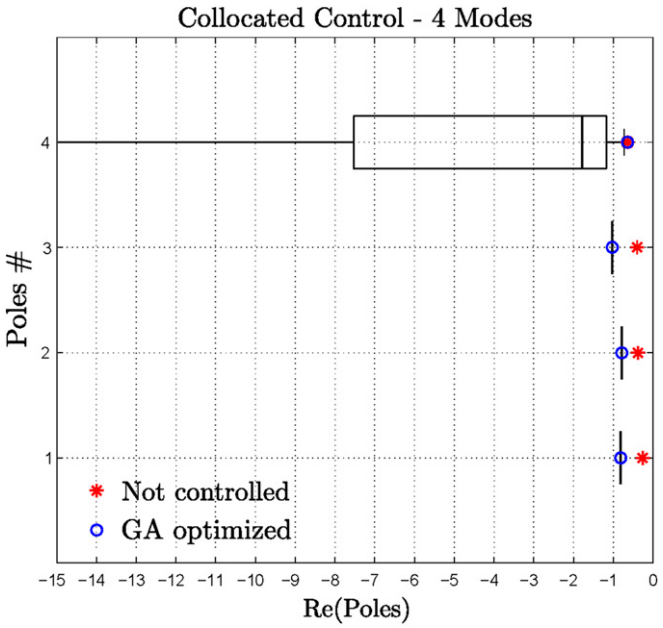

Figure 1. Test 1 ($n = 4$, $n_C = 3$, $\xi_C = \xi_M$). The effects of IMSC on the poles of the real system. The box-plot diagram represents the distribution of the poles when the sensors and actuators are placed randomly (median, 25th and 75th percentiles, non-outliers shown by whiskers).

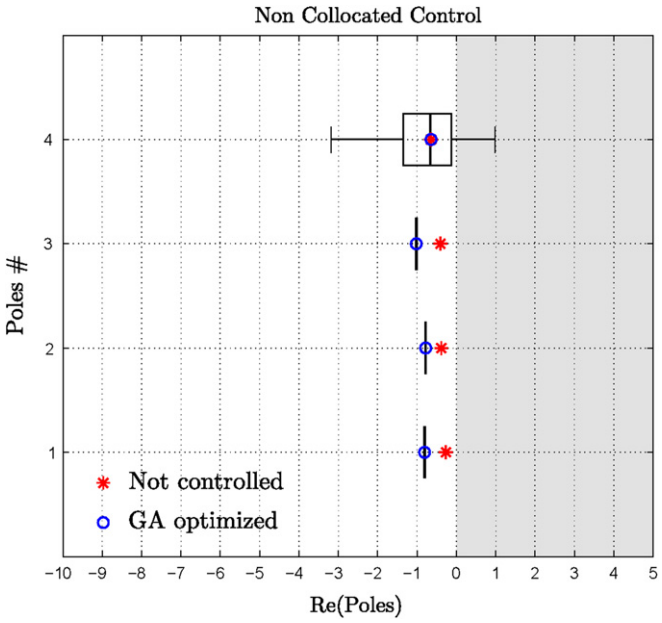

Figure 3. Test 2 ($n = 4$, $n_C = 3$, $\xi_C \neq \xi_M$). The effects of IMSC on the poles of the real system. The box-plot diagram represents the distribution of the poles when the sensors and actuators are placed randomly (median, 25th and 75th percentiles, non-outliers shown by whiskers).

5.2. Test 2—(n = 4) non-collocated control

The effects of optimization can also be observed when the control in non-collocated. Figure 3 shows the real part of the poles of both the uncontrolled and controlled systems with genetic algorithm optimization. Even for this case, whenever the optimization algorithm is used, the pole of the unmodeled mode remains unchanged. As seen in figure 4, the sensors and actuators are placed on the nodes of the unmodeled mode, thus avoiding any contribution to thr measurements and control forces on that mode. However, as this test considers non-collocated control, stability can not be guaranteed if arbitrary positions for the sensors and actuators are chosen.

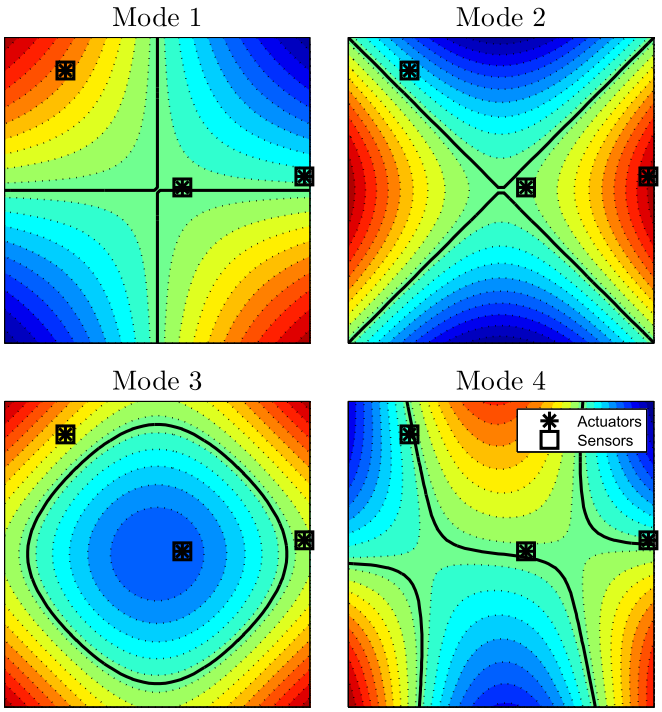

Figure 2. Test 1 ($n = 4$, $n_C = 3$, $\xi_C = \xi_M$). The optimal positions of the actuators and sensors, depicted over the first four modes.

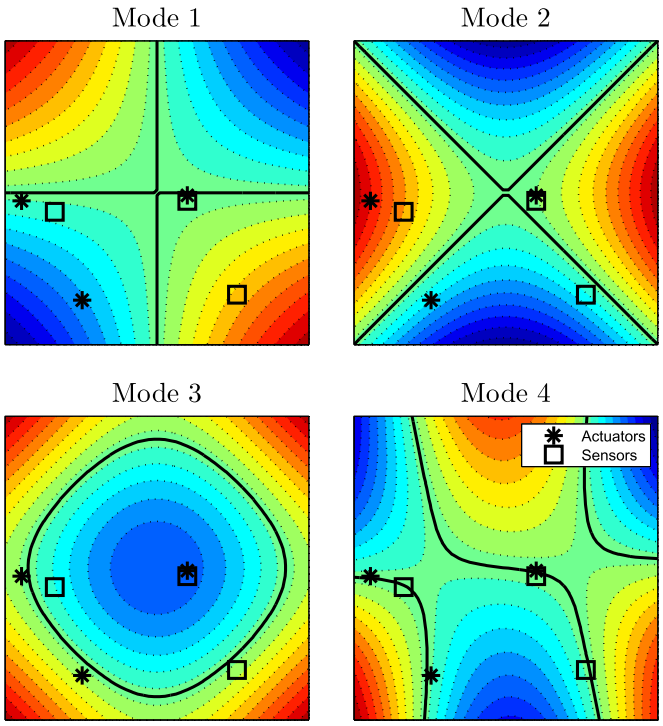

Figure 4. Test 2 ($n = 4$, $n_C = 3$, $\xi_C \neq \xi_M$). The optimal positions of the actuators and sensors, depicted over the first four modes.

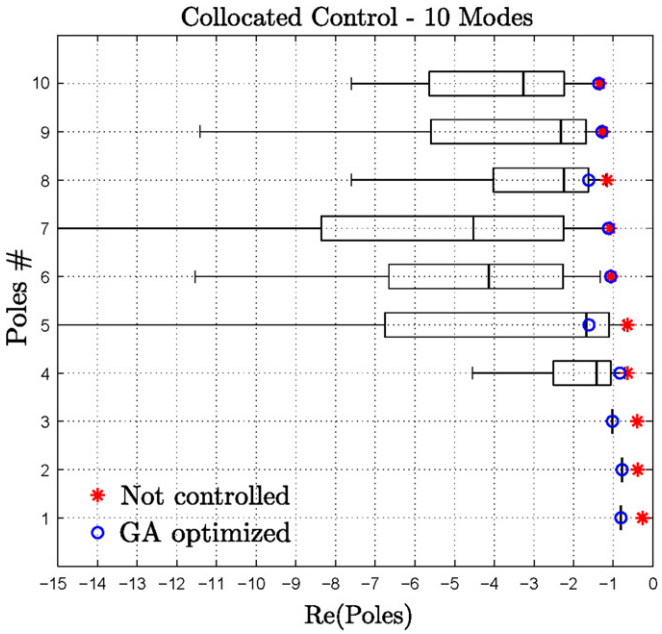

Figure 5. Test 3 ($n = 10$, $n_C = 3$, $\xi_C = \xi_M$). The effects of IMSC on the poles of the real system. The box-plot diagram represents the distribution of the poles when the sensors and actuators are placed randomly (median, 25th and 75th percentiles, non-outliers shown by whiskers).

Figure 3 shows how spillover effects can change the pole of the unmodeled mode, leading to a possible instability.

5.3. Test 3—(n = 10) collocated control

Let us consider the case of an extensive system ($n = 10$), where the three actuators required to perform IMSC are positioned in the same place as the sensors ($\xi_C = \xi_M$). In figure 5, it can be seen that the control acts on the first three modes of the system increasing their damping. Since the control is collocated the system is always stable. Even if the unmodeled modes are also modified by the control, spillover effects are limited as the poles of the unmodeled modes change only slightly. As a matter of fact, their position remains the same for many modes, whereas for others (i.e. modes 5, 8) the change still remains lower than the median value corresponding to a random placement of sensors and actuators. As the target of the optimization is to reduce the global effects of spillover, then it can be that a set of positions of sensors and actuators can be non-optimal for a given mode. Figure 6 shows the optimal positions of the sensors and actuators with respect to the first ten modal shapes of the structure.

5.4. Test 4—(n = 10) non-collocated control

Let us consider the case where the three actuators are not placed in the same positions as the sensors. Figure 7 shows the poles of both the uncontrolled and controlled systems. It can be noted that, as the control is non-collocated, some modeled modes can become unstable due to spillover effects. In contrast, the use of genetic algorithm optimization allows the position of the poles of most unmodeled modes to remain unchanged. Some modes are necessarily affected by the control (i.e. modes 4, 8), but the changes to their dynamics are small and the system continues to be stable. Figure 8 shows the optimal positions of the sensors and actuators with respect to the first ten modal shapes of the structure.

5.5. Results

The tests carried out show that the approach proposed in this paper can effectively minimize the effects of spillover. This is made possible first of all by being able to describe the relationship between these effects and the positions of the sensors and actuators.

Obviously, the performance of the algorithm significantly depends on the number of unmodeled modes. The performance has been evaluated by comparing optimal solutions with a significant number of random conditions (evaluating all the possible combinations would be impossible). This comparison can be performed easily for simple systems (tests 1 and 2), whereas for complex systems (tests 3 and 4) the optimization is more difficult. It is worth noting that, in all the cases, the optimization of the positions allows one to guarantee not only the stability, but also the effective decoupling between all the modes of the system (modeled and unmodeled), leaving the poles of the controlled system unchanged, as required by the IMSC technique.

For complex systems, such as the one considered, these results would not have been possible using the approaches proposed in [9, 16, 17] where, the mathematical complexity of the algorithms does not allow their practical use in real applications.

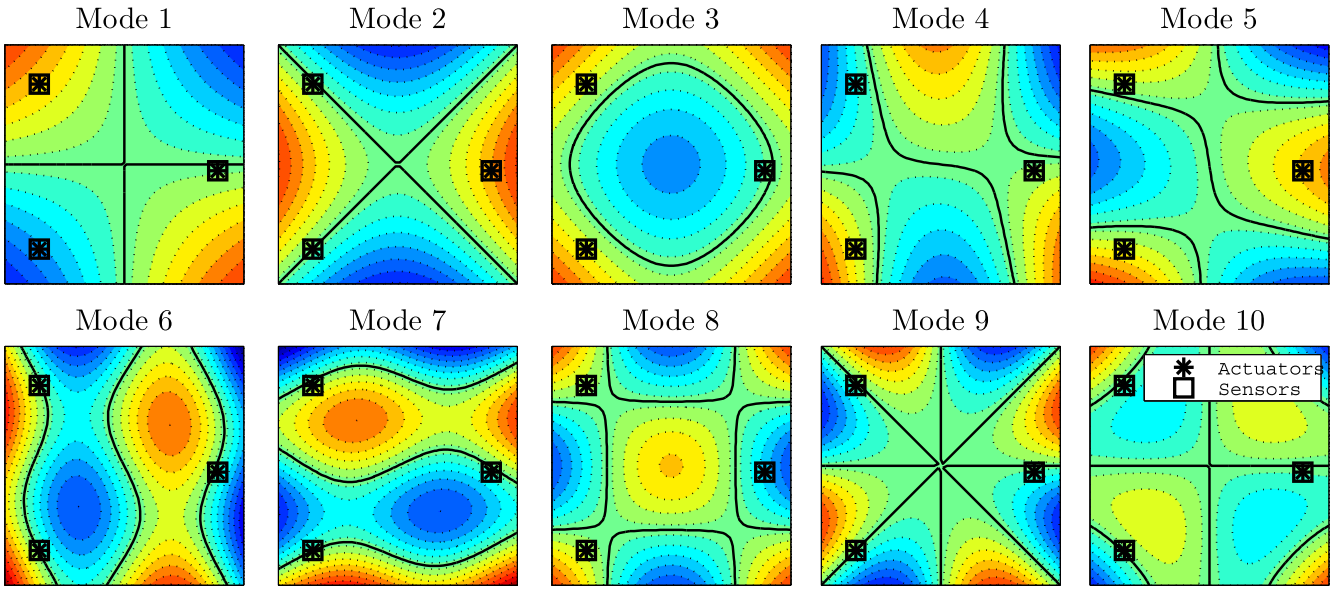

Figure 6. Test 3 (n = 10, n_C = 3, $\xi_C = \xi_M$). The optimal positions of the actuators and sensors, depicted over the first ten modes. The reduced model is based on the first three modes.

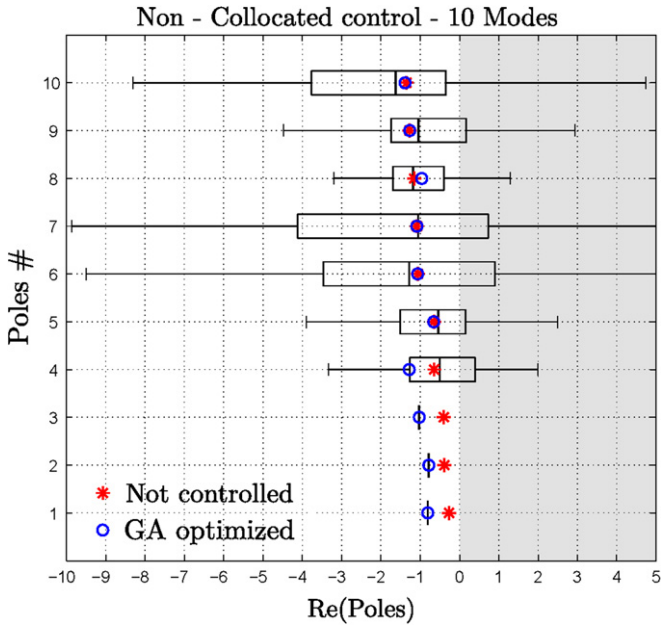

Figure 7. Test 4 (n = 10, n_C = 3, $\xi_C \neq \xi_M$). The effects of IMSC on the poles of the real system. The box-plot diagram represents the distribution of the poles when the sensors and actuators are placed randomly (median, 25th and 75th percentiles, non-outliers shown by whiskers).

Moreover, from a computational point of view, the optimization based on a genetic algorithm converges quickly. Table 2 compares the computational time required by the genetic algorithm versus trying all the combinations systematically ('c-l' stands for 'collocated'). While genetic algorithm optimization requires a small number of iterations to find the optimum, the brute force method requires $\binom{N}{n_R}$ operations for collocated control and $\binom{N}{2 \cdot n_R}$ for non-collocated control. In table 2 'iter' is the number of iterations of the genetic algorithm adopted, as explained in section 4. It is clearly apparent from table 2 that the genetic algorithm converges quickly to the best solution, compared to the brute force approach which checks each possible combination of the solution space, requiring vastly more time. The performed tests demonstrate how the adopted approach is satisfactory in the sense of keeping as constant the poles of the uncontrolled modes and placing the actuators for the control in the nodal lines of the uncontrolled modes. For test 1 and test 2, in addition to the different relative positions between the measuring and control devices, the position of the actuators over the nodal lines of the fourth mode, which is the only one not controlled, is clearly visible.

6. Experimental tests

The independent modal control technique was applied to a large flexible system consisting of a large, thin iron plate. The system is shown in figure 9: it consists of a 2 m × 2 m iron plate 10 mm in thickness, suspended from four steel wires. Modal identification of the system allows one to have the modal matrix $[\boldsymbol{\phi}]$ evaluated in the nodes of interest. Excitation and control forces are provided through inertial electromagnetic actuators.

A reduced model characterized by n_R = 3 modeled modes is considered. The reduced model suitably describes

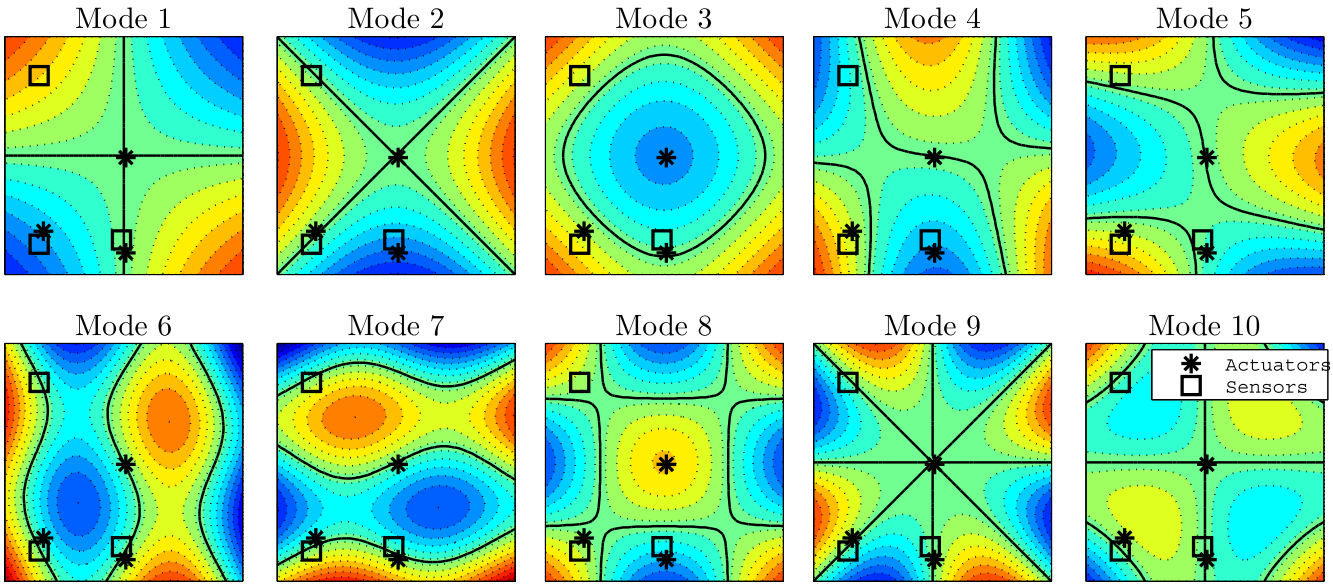

Figure 8. Test 4 ($n = 10$, $n_C = 3$, $\xi_C \neq \xi_M$). The optimal positions for the actuators and sensors, depicted over the first ten modes. The reduced model is based on the first three modes.

Figure 9. Experimental set-up.

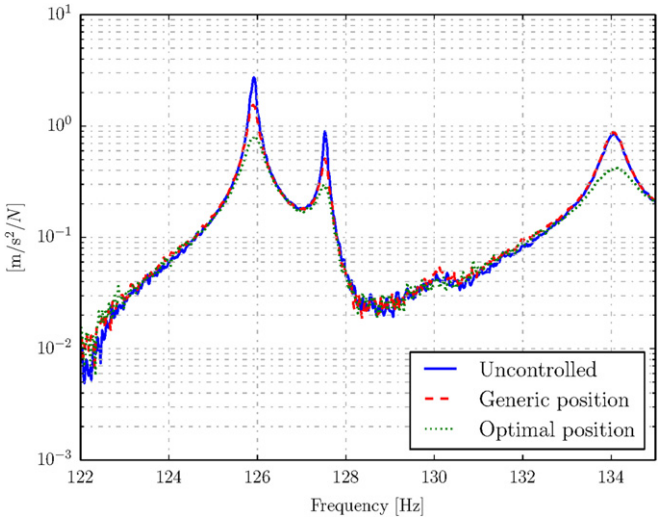

Figure 10. Vibration suppression for generic positions of sensors and actuators (dashed line) and optimal positions (dotted line).

the behavior of the real system in the range of frequencies $[120 : 135]$ Hz. According to IMSC requirements, three actuators and three sensors are used ($n_A = m = n_R = 3$) and a collocated configuration is considered. Figure 9 shows the experimental set-up. During tests, one actuator (marked by the letter D) provides a white noise band limited disturbance. The position of the actuator D and the amplitude of the disturbance are maintained as constant during the tests.

First, the sensors and actuators used to suppress vibration are placed in a generic position over the plate (marked by the letter C). Three accelerometers are placed under the plate in the same positions as the actuators ($\underline{\boldsymbol{\xi}}_M = \underline{\boldsymbol{\xi}}_C$). An independent modal controller is synthesized to reduce the vibrations associated with modeled modes increasing their corresponding modal damping. Gain is incrementally increased until the system is stable. When instabilities due to spillover effects occur, the test is stopped.

Table 2. The performance of genetic algorithm optimization compared to the brute force method, ('c-l' and 'iter' stand, respectively, for 'iteration' and 'collocated').

Genetic algorithm optimization	
Time for 1 iter	0, 22 ms
Time for 10^5 iter	37 min
Brute force approach	
Time for 1 iter	0, 09 ms
Collocated control	$5 \cdot 10^9$ iter
Time for c-l control	5, 2 days
Non-collocated control	$2, 5 \cdot 10^{19}$ iter
Time for non-c-l control	$\rightarrow\infty$

Figure 10 depicts the accelerations measured by sensors when the system is uncontrolled (solid line) and when the control is switched on (dashed line) for a generic placement of sensors and actuators. Independent modal control allows us to increase the modal damping of each modeled mode to effectively reduce the vibration of the system. While the effect of the control is significant on the first two modes, both characterized by a small modal damping, changes in the third modeled mode are null. The same test was performed placing the sensors and actuators in the optimal positions obtained from genetic optimization. The results are depicted on the same graph by a dotted line. In this case, attenuation on the three modeled modes is higher thanks to reduced spillover effects and the damping introduced on the modeled modes is close to the maximum achievable value, as discussed in [27].

7. Conclusions

The main limits on the use of IMSC are related to spillover effects. This paper analytically demonstrates that, once the reduced model is defined, spillover effects only depend on the positions of the sensors and actuators. Unfortunately, when the system has a high number of unmodeled modes, the choice of their locations is extremely complex because, in addition to reducing the effects of spillover, system observability and controllability have to be ensured.

This work exploits the potential of genetic algorithms to minimize the effects of IMSC on unmodeled modes. A fitness function has been defined to take into account the effects of unmodeled modes on the dynamics of the controlled system, highlighting their dependency on the positions of the sensors and actuators. Such an approach overcomes the limitations of traditional techniques which are effective only for systems with a few unmodeled modes.

Numerical simulations have been carried out for different cases. For simple systems (i.e. those characterized by a reduced number of unmodeled modes) it is easy to demonstrate that the solution from the optimization is the best, as it allows one to completely cut out spillover effects. Conversely, for more complex systems (i.e. those characterized by a high number of unmodeled modes), this assessment is more difficult. In fact, in such situations there is no solution that completely cancels spillover effects, nor it is easy to determine the best solution as this would require enormous computing resources. However, although it is not easy to prove that the solution found is the best possible, it is shown, both numerically and experimentally, that it allows one to achieve a better performance compared to those obtained for a high number of random configurations of sensors and actuators.

References

[1] Balas M J 1978 Modal control of certain flexible dynamic systems *J. Control. Optimiz.* **16** 450–62

[2] Balas M J 1978 Feedback Control of Flexible Systems *IEEE Trans. Automatic Control AC* **23** 673–9

[3] Balas M J 1978 Active control of flexible systems *J. Optim. Theory Appl.* **25** 415–35

[4] Balas M J 1979 Direct velocity feedback control of large flexible structures *J. Guid. Control* **3** 252–3

[5] Cazzulani G, Ghielmetti C, Giberti H, Resta F and Ripamonti F 2011 A test rig and numerical model for investigating truck mounted concrete pumps *Autom. Constr.* **20** 1133–42

[6] Cazzulani G, Cinquemani S and Comolli L 2012 Enhancing active vibration control performances in a smart structure by using fiber Bragg gratings sensors *Proc. SPIE* **8345** 834530

[7] Cazzulani G, Cinquemani S, Comolli L and Gardella A 2012 Reducing vibration in carbon fiber structures with piezoelectric actuators and fiber Bragg grating sensors *Proc. SPIE* **8341** 83411P

[8] Cazzulani G, Cinquemani S, Comolli L and Resta F 2013 A quasi-modal approach to overcome FBG limitations in vibration control of smart structures *Smart Mater. Struct.* **22** 1–10

[9] Chang M I J and Soong T T 1980 Optimal controller placement in modal control of complex system *J. Math. Anal. Appl.* **75** 340–58

[10] Falourd X, Lissek H and Rene P J 2009 Active low frequency modal noise cancellation for room acoustics: an experimental study *Proc. XVI Int. Congr. on Sound and Vibration (Krakow)* pp 5–9

[11] Fang J Q, Li Q S and Jeary A P 2003 Modified independent modal space control of m.d.o.f. systems *J. Sound Vib.* **261** 421–41

[12] Goldberg D E 1989 *Genetic Algorithms in Search Optimization and Machine Learning* (Reading, MA: Addison-Wesley)

[13] Conn A R, Gould N I M and Toint P L 1997 A globally convergent Lagrangian barrier algorithm for optimization with general inequality constraints and simple bounds *Math. Comput.* **66** 261–88

[14] Giberti H and Ferrari D 2014 A genetic algorithm approach to the kinematic synthesis of a 6-dof parallel manipulator *ESDA 2014: Proc. ASME 2014 12th Biennial Conf. on Engineering Systems, Design and Analysis (Copenhagen)*

[15] Hurlebaus S, Stobener U and Gaul L 2008 Vibration reduction of curved panels by active modal control *Comput. Struct.* **86** 251–7

[16] Ibidapo-Obe O 1985 Optimal actuators placements for the active control of flexible structures *J. Math. Anal. Appl.* **105** 12–25

[17] Ibidapo-Obe O 1986 Active control performance enhancement for reduced-order models of large-scale system *J. Math. Anal. Appl.* **120** 13–24

[18] Khulief Y A 1985 Vibration suppression in rotating beams using active modal control *J. Sound Vib.* **242** 681–99

[19] Meirovitch L and Oz H 1980 Modal-space control of large flexible spacecraft possessing ignorable coordinates *J. Guid. Control* **3** 569–77

[20] Meirovitch L, Baruh H and Oz H 1983 A comparison of control techniques for large flexible systems *J. Guid. Control* **6** 302–10

[21] Meirovitch L and Baruh H 1983 The implementation of modal filters for control of structures *J. Guid. Control Dyn.* **8** 707–16

[22] Meirovitch L 1990 *Dynamics and Control of Structures* (Hoboken, NJ: Wiley Interscience)

[23] Preumont A, Francois A, de Man P and Piefort V 2003 Spatial filter in structural control *J. Sound Vib.* **265** 61–79

[24] Preumont A, Francois A, de Man P, Loix N and Henrioulle K 2005 Distributed sensors with piezoelectric films in design of spatial filters for structural control *J. Sound Vib.* **282** 701–12

[25] Sang-Myeong K and Jae-Eung O 2013 A modal filter approach to non-collocated vibration control of structures *J. Sound Vib.* **332** 2207–21

[26] Weng M C, Lu X and Trumper D L 2002 Vibration control of flexible beams using sensor averaging and actuator averaging methods *IEEE Trans. Control Syst. Technol.* **1084** 568–77

[27] Elliott S J, Serrand M and Gardonio P 2001 Feedback stability limits for active isolation systems with reactive and inertial actuators *J. Vib. Acoust.* **123** 250–61